



## Short Communication

## Identification and characterization of Zika virus NS5 RNA-dependent RNA polymerase inhibitors

Yuan Lin<sup>a,1</sup>, Hongjuan Zhang<sup>a,1</sup>, Weibao Song<sup>a</sup>, Shuyi Si<sup>b</sup>, Yanxing Han<sup>a,\*</sup>, Jiandong Jiang<sup>a,b,\*\*</sup><sup>a</sup> State Key Laboratory of Bioactive Substances and Function of Natural Medicine, Institute of Materia Medica, Chinese Academy of Medical Sciences and Peking Union Medical College, Beijing, China<sup>b</sup> Institute of Medicinal Biotechnology, Chinese Academy of Medical Sciences and Peking Union Medical College, Beijing, China

## ARTICLE INFO

## Article history:

Received 16 December 2018

Accepted 10 July 2019

Editor: Philippe Colson

## Keywords:

Zika virus

NS5

RNA-dependent RNA polymerase

Inhibitor

## ABSTRACT

The current outbreak of Zika virus (ZIKV) is the impetus for novel, safe and efficacious anti-ZIKV agents. ZIKV non-structural protein 5 RNA-dependent RNA polymerase (RdRp) is essential for viral replication and is logically regarded as an attractive drug target. This study used a fluorescence-based polymerase assay to find an anti-infective drug 10-undecenoic acid zinc salt (UA) which could inhibit RdRp activity with a half maximal inhibitory concentration (IC<sub>50</sub>) of 1.13–1.25 μM. Molecular docking and site-directed mutagenesis analyses identified D535 as the key amino acid in the interaction between RdRp and UA. Importantly, the surface plasmon resonance assay showed that UA had strong direct binding with ZIKV wild-type RdRp and a relatively weak interaction with D535A-RdRp. As a control, the nucleoside inhibitor sofosbuvir triphosphate (PSI-7409) conferred insensitivity to the fluorescence-based RdRp assay and cannot bind directly with RdRp. Moreover, UA showed anti-ZIKV activity comparable to sofosbuvir. All these results indicate that UA is likely to be a promising lead compound against ZIKV, exhibiting a different mechanism than sofosbuvir.

© 2019 Elsevier B.V. and International Society of Chemotherapy. All rights reserved.

## 1. Introduction

Zika virus (ZIKV) causes neurological injury and congenital brain impacts when women are infected during pregnancy. The explosive spread of ZIKV through the Americas has caused worldwide attention and promoted the World Health Organization to declare ZIKV a global public health emergency. However, there are no vaccines or drugs for the prevention or treatment of ZIKV infection [1]. It may be a challenge to develop anti-ZIKV agents.

ZIKV is a single-stranded positive-sense RNA encoding a polyprotein of ~3400 amino acids. This polyprotein includes three structural proteins (C, prM and E) and seven non-structural (NS) proteins (NS1, NS2a, NS2b, NS3, NS4a, NS4b and NS5) [2]. NS5 is the largest enzyme and the most conserved protein component. It contains a methyltransferase (MT) domain at its N-terminus and an RNA-dependent RNA polymerase (RdRp) domain at its C-terminus.

The NS5 MT domain methylates the RNA cap to form N7-methylguanosine and 2'-O-methyl adenosine [3]. The NS5 RdRp domain carries out viral RNA synthesis through a de-novo initiation mechanism and is responsible for synthesizing RNA copies of both plus and minus polarity [4]. Since NS5 RdRp is absent in mammalian hosts and essential for viral replication, it is a significant drug target for anti-ZIKV agents.

For viral RdRp inhibitors, both nucleoside polymerase inhibitors (NIs) and non-nucleoside polymerase inhibitors (NNIs) have been approved in the case of viral infections [5]. NIs, when converted into a triphosphate form, can compete with natural NTP substrates and terminate the RNA chain elongation. Sofosbuvir was the first anti-HCV NI to achieve clinical success. The active chemical composition of sofosbuvir is phosphorylated intracellularly to 2'-C-methyl-2'-fluoro-uridine-5'-triphosphate (UTP) (PSI-7409), which binds at the active site of RdRp to compete with natural substrates for RNA synthesis [6]. NNIs usually bind with RdRp, either inactivating the enzyme or preventing the conformational changes required for RNA synthesis. For NNIs, both metal chelating agents and allosteric inhibitors have been shown to be successful for suppressing RdRp [7].

This study found that 10-undecenoic acid zinc salt (UA) could inhibit ZIKV RdRp by binding to its active centre D535 with poten-

\* Co-corresponding author. Address: Tel.: +86 10 63017906; fax: +86 10 63017906.

\*\* Corresponding author. Address: Tel.: +86 10 83160005; fax: +86 10 63017757.

E-mail addresses: [hanyanxing@imm.ac.cn](mailto:hanyanxing@imm.ac.cn) (Y. Han), [jiang.jdong@163.com](mailto:jiang.jdong@163.com)

(J. Jiang).

<sup>1</sup> These two authors contributed equally to this article.

tial anti-ZIKV activity. UA has a different mechanism of action than the approved clinical drug sofosbuvir, which may make it a potent anti-ZIKV agent.

## 2. Materials and methods

### 2.1. ZIKV NS5 RdRp activity assay

The cDNA sequence of ZIKV NS5 RdRp (nucleotides 8419–10374; KU321639.1) was synthesized *de novo* by Invitrogen (Waltham, MA, USA). NS5 wild-type (WT)-RdRp, D535A-RdRp and D692A-RdRp proteins were purified as described [8]. The RNA template, 3'UTR-A<sub>30</sub> (5'-A<sub>30</sub>-AACAGGUUCUAGAACCUGUU-3') was resuspended to 200 μM in a buffer consisting of 50 mM Tris-HCl (pH 8.0) and 150 mM NaCl in 0.1% diethyl pyrocarbonate water. The solution was incubated at 55–60°C for 5 min and placed at room temperature to allow formation of the intramolecular hairpin. The NS5 RdRp activity assay was performed in a 30-μL reaction mixture containing reaction buffer (50 mM Tris-HCl, pH 7.0, 2 mM dithiothreitol, 10 mM KCl and 1 mM MnCl<sub>2</sub>), 50 nM RNA template, 2 μM modified nucleotide analogue (2'-[2-benzothiazoyl]-6'-hydroxybenzothiazole) conjugated adenosine triphosphate (BBT-ATP) and 50 nM NS5 RdRp protein in a half-96-well black plate. The reaction was terminated by the addition of stop buffer (200 mM NaCl, 25 mM MgCl<sub>2</sub>, 1.5 M deoxyethanolamine) containing 25 nM calf intestinal alkaline phosphatase (CIAP). The released BBT was monitored at excitation/emission (ex/em) of 430/560 nm after 1 h of incubation [9,10].

### 2.2. ZIKV NS5 RdRp inhibitor screening

An anti-infection compound library of approximately 500 compounds, including drugs approved by the Food and Drug Administration (FDA) (MedChem Express, Monmouth Junction, NJ, USA), was screened. Briefly, the compound (10 μM) was pre-incubated with RdRp at room temperature for 0.5 h. Then, the inhibitory activity of the compound against RdRp was assayed as described above. The half maximal inhibitory concentration (IC<sub>50</sub>) of active compound (0.05–200 μM, two-fold dilution) was determined based on the ratio of light ex/em units over the concentration of compounds (log plots) fitted to a variable-slope dose–response equation. 3'-dATP, 3'-dUTP and sofosbuvir were used as reference compounds.

### 2.3. Molecular docking

Discovery Studio 2018R2 software (Accelrys, San Diego, CA, USA) was used for the in-silico analysis. The crystal structure of NS5 was retrieved from the Protein Data Bank (PDB ID: 5UOC) [2]. The docking pocket was chosen based on the active site reported, corresponding to D535, D665 and D666. To examine the molecular docking of UA and RdRp, two conformations of the UA structure were generated after optimization. Docking was carried out using the C-DOCKER program.

### 2.4. Surface plasmon resonance assay

Measurements were performed using a BIACore T200 (Uppsala, Sweden) at 25°C in PBS-T running buffer (PBS containing 0.05% Tween 20 and 0.1% DMSO). RdRp was coated on to a CM5 chip using an NHS/EDC amine coupling kit in 10 mM sodium acetate buffer at pH 4.5. To determine the binding effect of UA and WT-RdRp, various concentrations ranging from 0 to 12 μM UA were injected on to the WT-NS5 RdRp immobilized chip. The interaction of UA and WT-RdRp was represented by response units (RU). The equilibrium dissociation constant (*k<sub>D</sub>*) value was determined with

the BIACore evaluation software package. The interaction of D535A-RdRp with UA was examined using the same method. In addition, the interaction of 3'-dATP or PSI-7409 with WT-RdRp was analysed as a control.

### 2.5. Virus yield reduction assay

Virus yield reduction assay was performed by quantitative reverse transcription polymerase chain reaction using total RNA extracted from culture supernatants of Huh7 cells infected by ZIKV (SMGC-1) with 0.01–62.5 μM UA or sofosbuvir as described. Chloroquine, another FDA-approved drug with potent anti-ZIKV activity, was also used as a control [11].

## 3. Results

ZIKV NS5 RdRp protein was purified (Fig. 1A). A fluorescence-based alkaline phosphatase-coupled polymerase assay was used to characterize RdRp activity. RdRp catalyses nucleotidyl transfer of adenosine-5' monophosphate from BBT-ATP to the RNA chain, generating BBT-ppi that is subsequently hydrolysed to the fluorescent BBT. Measurement of the fluorescent BBT indirectly represented RdRp activity. As shown in Fig. 1B, WT-RdRp showed strong activity with noticeable FLU 430/560 nm signals. The polymerase activity increased as the reaction time extended.

To find the inhibitor of ZIKV NS5 RdRp, the BBT-ATP-coupled polymerase assay was used to screen the compound library. UA (Fig. 1C) was found to be potent against WT-RdRp activity with an IC<sub>50</sub> of 1.13 μM (Table 1). Two known RNA chain terminators, 3'-dATP and 3'-dUTP, were used as reference compounds. 3'-dATP was more potent than UA (IC<sub>50</sub> 0.11 μM). 3'-dUTP did not inhibit the polymerase activity (IC<sub>50</sub> >200 μM), indicating that the assay was specific to the reaction using adenosine triphosphate as nucleotide substrate. To further compare their inhibitory effects, the nucleotide substrates were changed from BBT-ATP to BBT-UTP. As expected, 3'-dUTP inhibited the NS5 RdRp with an IC<sub>50</sub> of 1.17 μM, while 3'-dATP had no inhibitory effect (IC<sub>50</sub> >200 μM). UA exhibited notable inhibition in this reaction (IC<sub>50</sub> 1.25 μM), which was almost the same value (1.13 μM) as when using BBT-ATP as the nucleotide substrate. However, PSI-7409 (the active 5'-triphosphate metabolite of sofosbuvir) did not inhibit the polymerase reaction using both BBT-ATP (IC<sub>50</sub> >200 μM) and BBT-UTP (IC<sub>50</sub> 83.54 μM) as the nucleotide substrate. All the results indicated that UA could strongly inhibit RdRp, and possesses a different mechanism than NIs (sofosbuvir, 3'-dATP and 3'-dUTP).

To identify the inhibitory mechanism of UA on RdRp, molecular docking was performed using Discovery Studio 2018R2 software. Fig. 1D showed that UA was located in the active site of NS5 RdRp, which coordinated with residues D535, D665 and D666. The interaction between UA and NS5 RdRp involved two amino acid residues: D535 and C667. The oxygen atom of the hydroxyl group of UA formed a conventional hydrogen bond with D535. In addition, an alkyl interaction bond between C11 of the UA carbon chain and C667 was observed (Fig. 1E).

Based on the molecular docking results, the key residue D535 was mutated to A535, and D692 located outside of the active site was mutated to A692. The mutant proteins were named 'D535A-RdRp' and 'D692A-RdRp', respectively. The polymerase activity of D535A-RdRp diminished largely compared with WT-RdRp, while the control D692A-RdRp retained almost the same activity as WT-RdRp (Fig. 1B).

To determine the inhibitory mechanism of UA, the polymerase activity was evaluated using D535A-RdRp and D692A-RdRp. In the BBT-ATP-based polymerase assay, the IC<sub>50</sub> values of UA for D535A-RdRp and D692A-RdRp were 21.33 and 1.79 μM, respectively

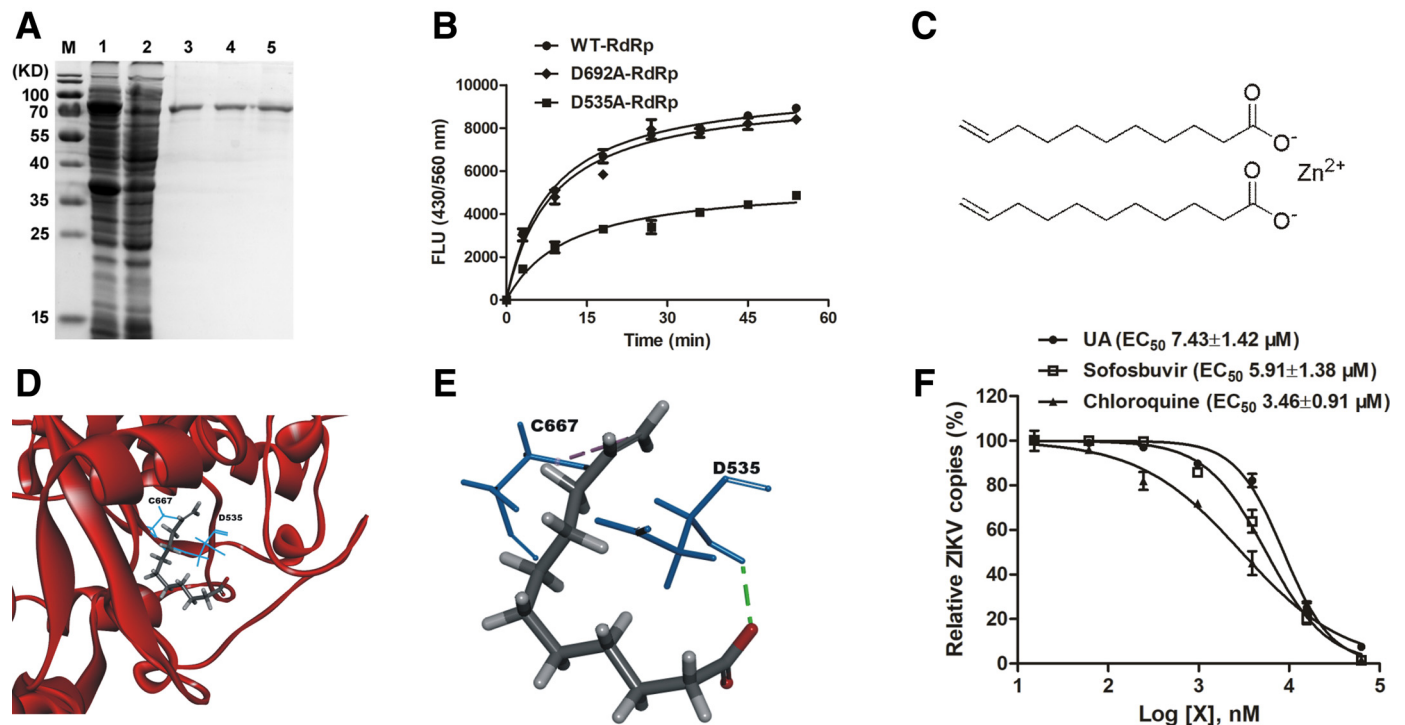


**Fig. 1.** Docking of 10-undecenoic acid zinc salt (UA) with active non-structural protein 5 (NS5) RNA-dependent RNA polymerase (RdRp) and anti-Zika virus (ZIKV) activity of UA. (A) Purification of NS5 RdRp and its mutants. Lane M, protein marker. Lane 1, induced total proteins of recombinant wild-type (WT)-RdRp. Lane 2, cellular lysate of induced recombinant WT-RdRp supernatant. Lane 3, purified recombinant WT-RdRp. Lane 4, purified recombinant D535A-RdRp. Lane 5, purified recombinant D692A-RdRp. (B) Activity of recombinant WT-RdRp, D535A-RdRp and D692A-RdRp. The fluorescence-based alkaline phosphatase-coupled polymerase assay was used. The polymerase reaction was initiated by mixing NS5 RdRp with 2'-[2-benzothiazoyl]-6'-hydroxybenzothiazole conjugated adenosine triphosphate (BBT-ATP) and RNA in the assay buffer. During the reaction, adenosine monophosphate was incorporated into RNA, leaving BBT<sub>ppi</sub> as a product of the reaction. Subsequent treatment of calf intestinal alkaline phosphatase (CIAP) in the reaction terminated NS5 RdRp activity and generated fluorescent BBT from BBT<sub>ppi</sub>. Then, 50 nM 3'UTR-A<sub>30</sub> and 2 μM BBT-ATP were incubated with 50 nM WT-RdRp (or D535A-RdRp and D692A-RdRp, respectively). The reaction was terminated by 25 nM CIAP. The released BBT was monitored at excitation/emission of 430/560 nm after 1 h of incubation. The experiment was repeated three times. (C) Structure of UA. (D) Molecular docking of UA and ZIKV NS5 RdRp. The active pocket of ZIKV NS5 RdRp was bound to UA. UA is represented by a stick model (grey, carbon atoms; deep red, oxygen atoms). The blue sticks represent the amino acids interacting with UA. (E) The detailed intermolecular bonds between ZIKV NS5 RdRp and UA. The hydrogen bond between D535 and the oxygen atom of UA is in green. The purple bond represents an alkyl interaction between C667 of ZIKV NS5 RdRp and C11 of UA carbon chain. (F) Inhibition of UA on ZIKV replication determined by quantitative reverse transcription polymerase reaction. Huh7 cells were infected by ZIKV with 0.01–62.5 μM UA. The relative levels of viral RNA in UA-treated cells were calculated as the percentage of that of untreated ZIKV-infected cells. Sofosbuvir and chloroquine were used as controls. Half maximal effective concentration (EC<sub>50</sub>) values were calculated from dose–response curves in three independent experiments using GraphPad 5.0. Data are shown as mean ± standard deviation.

**Table 1**  
Inhibition of various compounds in the 2'-[2-benzothiazoyl]-6'-hydroxybenzothiazole conjugated adenosine triphosphate (BBT-ATP)-coupled/BBT-uridine-5'-triphosphate (UTP)-coupled Zika virus non-structural protein 5 (NS5) RNA-dependent RNA polymerase (RdRp) assay.

Compound	IC <sub>50</sub> (μM) <sup>a</sup>					
	BBT-ATP-coupled assay			BBT-UTP-coupled assay		
	WT-RdRp	D535A-RdRp	D692A-RdRp	WT-RdRp	D535A-RdRp	D692A-RdRp
UA	1.13 ± 0.24	21.33 ± 3.52	1.79 ± 0.58	1.25 ± 0.36	28.74 ± 3.35	1.76 ± 0.13
3'-dATP	0.11 ± 0.07	0.16 ± 0.08	0.15 ± 0.04	>200	-	-
3'-dUTP	>200	-	-	1.17 ± 0.15	1.34 ± 0.48	1.29 ± 0.35
PSI-7409	>200	-	-	83.54 ± 6.66	92.95 ± 6.28	88.22 ± 7.71

IC<sub>50</sub>, half maximal inhibitory concentration; UA, 10-undecenoic acid zinc salt; WT, wild-type.

<sup>a</sup> GraphPad Prism 5.0 program was used to calculate IC<sub>50</sub> as well as best-fit curves. Each assay was performed in triplicate.

(Table 1). A 20-fold IC<sub>50</sub> value for D535A-RdRp was observed in comparison with WT-RdRp. In contrast, the inhibition of 3'-dATP to WT and mutant RdRp (D535A-RdRp and D692A-RdRp) was nearly unchanged (IC<sub>50</sub> 0.11, 0.16 and 0.15 μM, respectively). Similar results were observed in the BBT-UTP-based polymerase assay. In brief, the IC<sub>50</sub> values of UA against D535A-RdRp and D692A-RdRp were 28.74 and 1.76 μM, respectively. The inhibition of 3'-dUTP to WT and mutant RdRp was nearly unchanged (IC<sub>50</sub> 1.17, 1.34 and 1.29 μM, respectively). As expected, 3'-dATP had no inhibitory effect (IC<sub>50</sub> >200 μM) on WT and mutant RdRp in the BBT-UTP-based polymerase assay. Interestingly, the IC<sub>50</sub> values of PSI-7409

against WT and mutant RdRp were almost the same (IC<sub>50</sub> 83.54, 92.95 and 88.22 μM, respectively).

As surface plasmon resonance (SPR) is widely used for measuring interactions between proteins and small molecules, it was suitable to detect the direct interaction of UA and ZIKV NS5 RdRp. As evidenced by a measurable change in RU, UA was able to bind with WT-RdRp in a dose-dependent (0–12 μM) manner (Fig. 2A). *k<sub>D</sub>* was 0.3 μM. When D535A-RdRp was used as an analyte, the RU was considerably lower than for WT-RdRp (Fig. 2B). The *k<sub>D</sub>* for binding of UA to D535A-RdRp was 12 μM, a 40-fold increase compared with WT-RdRp. This result confirmed that D535 played

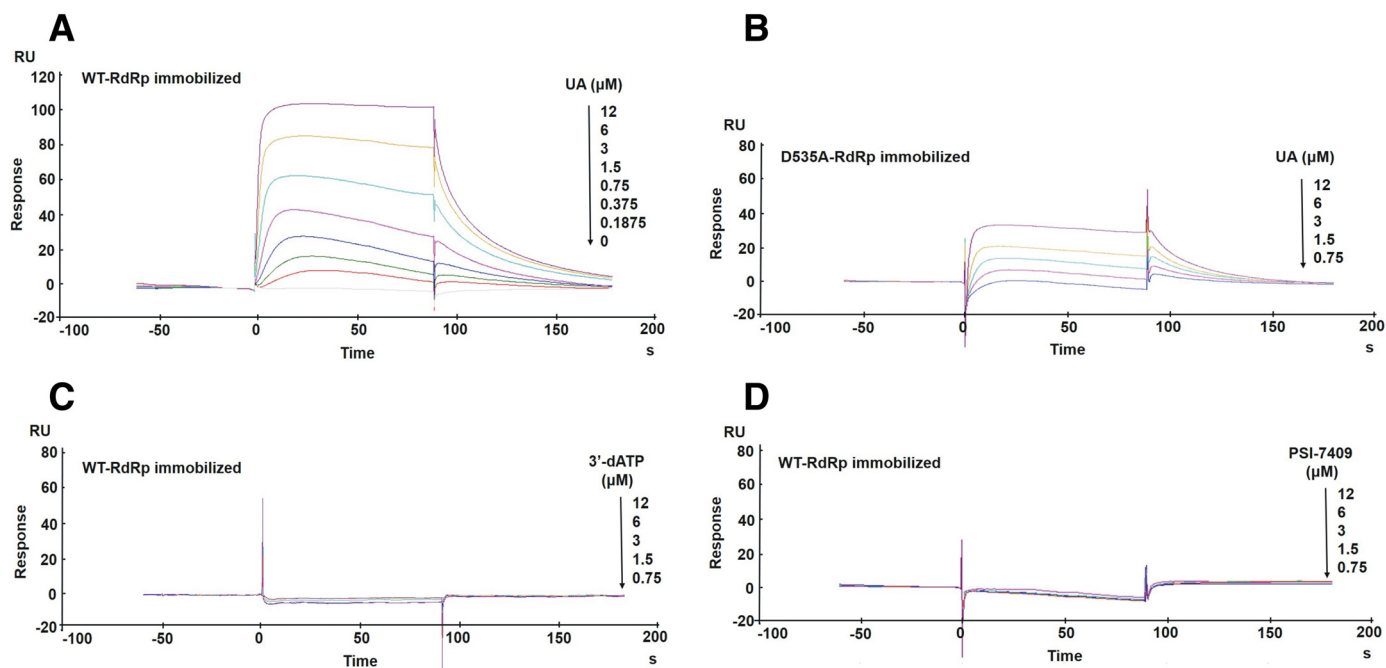


**Fig. 2.** Surface plasmon resonance analysis for the binding of 10-undecenoic acid zinc salt (UA), 3'-dATP and sofosbuvir triphosphate PSI-7409 to Zika virus non-structural protein 5 (NS5) RNA-dependent RNA polymerase (RdRp) and its mutants. (A, C, D) Binding of UA (A), 3'-dATP (C) and PSI-7409 (D) to wild-type (WT)-RdRp protein. Various concentrations (0–12  $\mu\text{M}$ ) of UA (A), 3'-dATP (C) or PSI-7409 (D) were injected into the chamber with a WT-RdRp-coated sensor chip. The change of response units (RU) is shown. (B) Binding of UA to D535A-RdRp protein.

an essential role in the interaction of UA with RdRp. Interestingly, both 3'-dATP and PSI-7409 (NIs) failed to bind with WT-RdRp (Fig. 2C and 2D). Therefore, UA may interfere with RdRp activity and RNA synthesis by binding directly to RdRp via the key amino acid D535.

In the virus yield reduction assay, UA, sofosbuvir and chloroquine reduced infectious virus yield in Huh7 cells with half maximal effective concentrations ( $\text{EC}_{50}$ ) of  $7.43 \pm 1.42$ ,  $5.91 \pm 1.38$  and  $3.46 \pm 0.91$   $\mu\text{M}$ , respectively (Fig. 1F). In addition, the  $\text{IC}_{50}$  of UA using an MTT assay in Huh7 cells was  $>100$   $\mu\text{M}$ , indicating that the anti-ZIKV activity was not caused by compound-induced cytotoxicity. Together, these results indicated that UA could reduce ZIKV replication by inhibiting RdRp activity, and possesses a different mechanism than sofosbuvir.

#### 4. Discussion

Currently, there are several effective ZIKV inhibitors, such as envelope glycoprotein inhibitor nanchangmycin, NS2B/NS3 protease inhibitor temoporfin, NS3 helicase inhibitor suramin and NS5 RdRp inhibitor sofosbuvir [8,12]. Although considerable efforts have been made to discover anti-ZIKV drugs, no approved drugs are available to date in the clinic. Many of the compounds were unsuitable for clinical use because of their high inhibition concentration to ZIKV or their cytotoxicity.

NS5 RdRp was a promising drug target and has been identified by a large number of NIs and NNIs available for the treatment of human immunodeficiency virus, hepatitis B virus and hepatitis C virus (HCV) [5]. Sofosbuvir was the most successful NI for the treatment of HCV. However, its toxicity and the complication of being a prodrug (converting to a triphosphate form of NIs) make it a little challenging. In addition, direct substrate-binding sites and allosteric regulation sites have gained attention for developing NNIs [13]. For ZIKV NS5 RdRp, the crystal structure has been reported recently [2,4], which helps identify suitable drug target sites and elucidates the drug-binding features. The main catalytic

centre of RdRp contains three aspartates (D535, D665 and D666) associated with the positioning of two metal ions mediating nucleotide transfer. For ZIKV NS5 RdRp NNIs, a pharmacophore-based in-silico drug screening was used to search for RdRp inhibitors [14]. ZINC39563464 showed the best docking score and its inhibition activity remains to be confirmed. Another study using a repurposing strategy identified that DMB213 was an inhibitor of RdRp with an  $\text{IC}_{50}$  of 5.2  $\mu\text{M}$  [9]. DMB213 is a pyridoxine-derived small molecular compound chelating the divalent metal ions from the catalytic site of RdRp [15]. The present study showed that UA inhibited RdRp activity with a comparatively low  $\text{IC}_{50}$  (1.13–1.25  $\mu\text{M}$ ) and interfered with RdRp activity by binding directly to the key amino acid D535. Compared with DMB213, UA exhibited a distinct inhibition mechanism. In addition, UA is the first NNI reported to bind with the active centre (D535) to inactivate RdRp.

A series of NIs were tested against ZIKV NS5 RdRp. The most efficient RdRp inhibitors were 2'-C-Me-UTP and 2'-C-ethynyl-UTP, with  $\text{IC}_{50}$  values of 5.78 and 0.46  $\mu\text{M}$ , respectively. Interestingly, 2'-F-2'-C-Me-UTP (PSI-7409) was not a potent inhibitor ( $\text{IC}_{50}$  90.76  $\mu\text{M}$ ) of RdRp [9]. Sacramento et al. reported that specifically modified UTPs (biotinylated-UTP and digoxigenin-UTP) rather than natural UTPs were used as competing 5'-triphosphates [16]. In the assay using biotinylated-UTP and digoxigenin-UTP, PSI-7409 inhibited RdRp with a low  $\text{IC}_{50}$  of 0.38  $\mu\text{M}$ , suggesting a different result when various UTPs were used. In the present study, the competing 5'-triphosphate for PSI-7409 was BBT-UTP with an  $\text{IC}_{50}$  of 83.54  $\mu\text{M}$ . This was in accordance with the assay using natural UTP. However, UA was a potent inhibitor when both BBT-ATP and BBT-UTP were used. This result suggests that UA possesses a different mechanism of action than PSI-7409.

In SPR analysis, 3'-dATP and PSI-7409 did not bind directly with WT-RdRp. The catalytic sites of NS5 RdRp are D535, D665 and D666, which are involved in the coordination of two divalent  $\text{Mg}^{2+}$  cofactors [15]. In addition,  $\text{Mn}^{2+}$  is essential for the RdRp assay [9]. 3'-dATP and PSI-7409 are likely to enter the catalytic site of RdRp and compete with the natural substrate NTPs, with divalent

metal ions indispensable. In the SPR assay, WT-RdRp was coated on the CM5 sensor chip without any metal ions. This may be the reason why 3'-dATP and PSI-7409 failed to bind with WT-RdRp. In contrast, UA could bind directly with WT-RdRp regardless of whether the ions were present. These data suggest that UA exhibits a distinct inhibition mechanism compared with 3'-dATP and PSI-7409.

UA is a fatty acid with various biological activities [17]. It has been reported that UA inhibited fungi with biofilm formation to prevent morphogenesis [18]. The derivatives of UA afforded broad-spectrum antibacterial activities [19]. Besides, UA has antiviral activity against herpes simplex virus [20]. However, there are no reports for anti-ZIKV activity with UA. UA is currently used as a systemic antifungal agent, with almost no cytotoxicity on human cells and an oral median lethal dose of 2.5 g/kg in rats [17]. Ingestion of UA and its derivatives are generally safe. Hopefully, further modification of UA holds promise to yield more effective anti-ZIKV drugs.

In conclusion, UA was found to inhibit ZIKV NS5 RdRp activity by binding with D535 of the active site. UA is the first NNI reported to bind directly with the active site of ZIKV NS5 RdRp, and exhibited anti-ZIKV activity with a distinct mechanism than sofosbuvir. Thus, this research might help to find new drug candidates against ZIKV and provide further insights into anti-ZIKV drug development.

#### Funding

This work was supported by the Zika Special Project of MOST (273-2016), NSFC (81773784), Beijing Nova Program (Z181100006218075), Basic Scientific Research Program of CAMS (2018RC350005), CAMS Major Collaborative Innovation Project (2016-I2M-1-011) and Drug Innovation Major Project (2018ZX09711001-002-002).

#### Declaration of Competing Interest

None declared.

#### Ethical approval

Not required.

#### References

- [1] Masmajan S, Baud D, Musso D, Panchaud A. Zika virus, vaccines, and antiviral strategies. *Expert Rev Anti Infect Ther* 2018;16:471–83.
- [2] Zhao B, Yi G, Du F, Chuang YC, Vaughan RC, Sankaran B, et al. Structure and function of the Zika virus full-length NS5 protein. *Nat Commun* 2017;8:14762.
- [3] Coutard B, Barral K, Lichiere J, Selisko B, Martin B, Aouadi W, et al. Zika virus methyltransferase: structure and functions for drug design perspectives. *J Virol* 2017;91:e02202–16.
- [4] Godoy AS, Lima GM, Oliveira KI, Torres NU, Maluf FV, Guido RV, et al. Crystal structure of Zika virus NS5 RNA-dependent RNA polymerase. *Nat Commun* 2017;8:14764.
- [5] Cheek MA, Sharaf ML, Dobrikov MI, Shaw BR. Inhibition of hepatitis C viral RNA-dependent RNA polymerase by alpha-P-boranophosphate nucleotides: exploring a potential strategy for mechanism-based HCV drug design. *Antiviral Res* 2013;98:144–52.
- [6] Liu J, Du J, Wang P, Nagarathnam D, Espiritu CL, Bao H, et al. A 2'-deoxy-2'-fluoro-2'-C-methyl uridine cyclopentyl carbocyclic analog and its phosphoramidate prodrug as inhibitors of HCV NS5B polymerase. *Nucleosides Nucleotides Nucleic Acids* 2012;31:277–85.
- [7] Netzler NE, Enosi Tuipulotu D, Eltahlia AA, Lun JH, Ferla S, Brancale A, et al. Broad-spectrum non-nucleoside inhibitors for caliciviruses. *Antiviral Res* 2017;146:65–75.
- [8] Xu HT, Hassounah SA, Colby-Germinario SP, Oliveira M, Fogarty C, Quan Y, et al. Purification of Zika virus RNA-dependent RNA polymerase and its use to identify small-molecule Zika inhibitors. *J Antimicrob Chemother* 2017;72:727–34.
- [9] Niyomrattanakit P, Abas SN, Lim CC, Beer D, Shi PY, Chen YL. A fluorescence-based alkaline phosphatase-coupled polymerase assay for identification of inhibitors of dengue virus RNA-dependent RNA polymerase. *J Biomol Screen* 2011;16:201–10.
- [10] Lu G, Bluemling GR, Collop P, Hager M, Kuiper D, Gurale BP, et al. Analysis of ribonucleotide 5'-triphosphate analogs as potential inhibitors of Zika virus RNA-dependent RNA polymerase by using nonradioactive polymerase assays. *Antimicrob Agents Chemother* 2017;61:e01967–16.
- [11] Delvecchio R, Higa LM, Pezzuto P, Valadao AL, Garcez PP, Monteiro FL, et al. Chloroquine, an endocytosis blocking agent, inhibits Zika virus infection in different cell models. *Viruses* 2016;8:322.
- [12] Gorshkov K, Shiryayev SA, Fertel S, Lin YW, Huang CT, Pinto A, et al. Zika virus: origins, pathological action, and treatment strategies. *Front Microbiol* 2018;9:3252.
- [13] Yokokawa F, Nilar S, Noble CG, Lim SP, Rao R, Tania S, et al. Discovery of potent non-nucleoside inhibitors of dengue viral RNA-dependent RNA polymerase from a fragment hit using structure-based drug design. *J Med Chem* 2016;59:3935–52.
- [14] Ramharack P, Soliman MES. Zika virus NS5 protein potential inhibitors: an enhanced in silico approach in drug discovery. *J Biomol Struct Dyn* 2018;36:1118–33.
- [15] Xu HT, Colby-Germinario SP, Hassounah S, Quashie PK, Han Y, Oliveira M, et al. Identification of a pyridoxine-derived small-molecule inhibitor targeting dengue virus RNA-dependent RNA polymerase. *Antimicrob Agents Chemother* 2016;60:600–8.
- [16] Sacramento CQ, de Melo GR, de Freitas CS, Rocha N, Hoelz LV, Miranda M, et al. The clinically approved antiviral drug sofosbuvir inhibits Zika virus replication. *Sci Rep* 2017;7:40920.
- [17] Brayden DJ, Walsh E. Efficacious intestinal permeation enhancement induced by the sodium salt of 10-undecylenic acid, a medium chain fatty acid derivative. *AAPS J* 2014;16:1064–76.
- [18] Helms S, Miller A. Natural treatment of chronic rhinosinusitis. *Altern Med Rev* 2006;11:196–207.
- [19] Rahman VP, Mukhtar S, Ansari WH, Lemiere G. Synthesis, stereochemistry and biological activity of some novel long alkyl chain substituted thiazolidin-4-ones and thiazan-4-one from 10-undecenoic acid hydrazide. *Eur J Med Chem* 2005;40:173–84.
- [20] Bourne N, Ireland J, Stanberry LR, Bernstein DI. Effect of undecylenic acid as a topical microbicide against genital herpes infection in mice and guinea pigs. *Antiviral Res* 1999;40:139–44.